current issues in molecular biology

MDPI

*Article*

# Establishment of A Novel Anti-CD44 Variant 10 Monoclonal Antibody $C_{44}$Mab-18 for Immunohistochemical Analysis against Oral Squamous cell carcinomas

**Kenichiro Ishikawa [1,#], Hiroyuki Suzuki [1,2,#*], Mika K. Kaneko [1,2] and Yukinari Kato [1,2,*]**

[1] Department of Molecular Pharmacology, Tohoku University Graduate School of Medicine, 2-1 Seiryo-machi, Aoba-ku, Sendai 980-8575, Japan; ken.ishikawa.r3@dc.tohoku.ac.jp (K.I.); k.mika@med.tohoku.ac.jp (M.K.K.)
[2] Department of Antibody Drug Development, Tohoku University Graduate School of Medicine, 2-1 Seiryo-machi, Aoba-ku, Sendai 980-8575, Japan
* Correspondence: hiroyuki.suzuki.b4@tohoku.ac.jp (H.S.); yukinari.kato.e6@tohoku.ac.jp (Y.K.); Tel.: +81-22-717-8207 (H.S. and Y.K.).
[#] contributed equally to this work

**Abstract:** Head and neck squamous cell carcinoma (HNSCC) is the most common type of head and neck cancer, and has been revealed as the second-highest expression of CD44 in cancers. CD44 has been investigated as a cancer stem cell marker of HNSCC and plays a critical role in tumor malignant progression. Especially, splicing variant isoforms of CD44 (CD44v) are overexpressed in cancers and considered a promising target for cancer diagnosis and therapy. We developed monoclonal antibodies (mAbs) against CD44 by immunizing mice with CD44v3–10-overexpressed PANC-1 cells. Among the established clones, $C_{44}$Mab-18 (IgM, kappa) reacted with CHO/CD44v3–10, but not with CHO/CD44s and parental CHO-K1 by flow cytometry. The epitope mapping using peptides that cover variant exon-encoded regions revealed that $C_{44}$Mab-18 recognized the border sequence between variant 10 and the constant exon 16-encoded sequence. These results suggest that $C_{44}$Mab-18 recognizes variant 10-containing CD44v, but not CD44s. Furthermore, $C_{44}$Mab-18 could recognize the human oral squamous cell carcinoma (OSCC) cell line, HSC-3 in flow cytometry. The apparent dissociation constant ($K_D$) of $C_{44}$Mab-18 for CHO/CD44v3–10 and HSC-3 was $1.6 \times 10^{-7}$ M and $1.7 \times 10^{-7}$ M, respectively. Furthermore, $C_{44}$Mab-18 detected CD44v3–10, but not CHO/CD44s in western blotting, and endogenous CD44v10 in immunohistochemistry using OSCC tissues. These results indicated that $C_{44}$Mab-18 is useful for detecting CD44v10 in flow cytometry and immunohistochemistry.

**Keywords:** CD44; CD44v10; monoclonal antibody; oral squamous cell carcinoma, immunohistochemistry

**Citation:** To be added by editorial staff during production.

Academic Editor: Firstname Lastname

Received: date
Revised: date
Accepted: date
Published: date



## 1. Introduction

Head and neck cancer is the seventh most common cancer type globally, and exhibits a profound impact on patients and their quality of life after surgical ablation and therapies [1]. Head and neck squamous cell carcinoma (HNSCC) is the most common type of head and neck cancer. The treatment of HNSCC includes surgery, chemotherapy, radiation therapy, immunotherapy, molecular targeted therapy, or a combination of those modalities [2]. Although survival can be improved by the development of treatments, cancer metastasis, and drug resistance remain the main causes of death [3]. The rate of 5-year survival remains stagnant at approximately 50% [4].

CD44 is a multifunctional type I transmembrane glycoprotein, which mediates metastasis and drug resistance in tumor cells. HNSCC is revealed as the second-highest

CD44-expressing tumor in the Pan-Cancer Atlas [5]. The alternative splicing of CD44 mRNA produces the various isoforms [6]. The constant exons including the first five (1 to 5) and the last five (16 to 20) are present in all variants and make up the standard isoform (CD44s). The CD44 variant (CD44v) isoforms are generated by the alternative splicing of variant exons (v1 to v10) in various combinations with the constant exons of CD44s [7]. Both CD44s and CD44v (pan-CD44) attach to the extracellular matrix including hyaluronic acid (HA) and facilitate the activation of metastasis-associated intracellular signaling pathways [8].

Tumor metastasis is a multistep process called the invasion-metastasis cascade, which includes (1) dissemination from primary sites, (2) the acquisition of migration/invasion phenotype, (3) intra/extravasation, (4) survival in circulation, and (5) adaptation and colonization in a distant organ [9]. Furthermore, (6) cancer associate fibroblasts and tumor-infiltrating lymphocytes in the tumor microenvironment involve in the promotion of tumor metastasis [10]. CD44 mediates the multiple steps of the invasion-metastasis cascade through interaction with HA [11] and CD44v-specific functions [12].

CD44 has been studied as a cell surface marker of cancer stem-like cells (CSCs) in various tumors [13]. Monoclonal antibodies (mAbs) against CD44s or CD44v are utilized to collect the CD44-high CSCs [13]. The CD44-high population exhibited the increased self-renewing property, drug resistance, and metastatic colonization *in vivo* [13]. CD44 is the first applied CSC marker to isolate HNSCC-derived CSCs [14]. Notably, CD44-high CSCs from HNSCC tumors showed the properties of epithelial to mesenchymal transition (EMT). The activation of the EMT program confers tumor cells the ability of migration, invasion, extravasation, and stemness [15]. Furthermore, CD44-high cells could make colonization in the lungs of immunodeficient mice, compared to CD44-low, which failed to form the metastatic colonization [16].

Furthermore, CD44v8–10 mediates the resistance to treatment. The v8–10-encoded region binds to and stabilizes a cystine–glutamate transporter (xCT), which enhances cystine uptake and glutathione synthesis [17]. The elevation of reduced glutathione (GSH) mediates the defense to reactive oxygen species (ROS) [17], radiation [18], and chemotherapeutic drugs [19]. The expression of CD44v8–10 is associated with the xCT function and redox status, and links to the poor prognosis of patients [18]. Therefore, the establishment of each CD44v-specific mAb is essential to reveal the function and develop CD44-targeting cancer therapy. However, the function or tissue distribution of the variant 10-encoded region has not been fully understood.

Using the Cell-Based Immunization and Screening (CBIS) method, our laboratory developed an anti-pan-CD44 mAb, $C_{44}$Mab-5 ($IgG_1$, kappa) [20]. By immunizing mice with CD44v3–10 ectodomain, another anti-pan-CD44 mAb, $C_{44}$Mab-46 [21] was established. Both $C_{44}$Mab-5 and $C_{44}$Mab-46 have the epitopes within the constant exon 2 and 5-encoding sequences [22-24] and apply to immunohistochemistry in oral squamous cell carcinomas (OSCC) [20] and esophageal SCC [21], respectively. Furthermore, we produced a class-switched and defucosylated type of recombinant $C_{44}$Mab-5 (5-m$G_{2a}$-f) using fucosyltransferase 8 (Fut8)-deficient ExpiCHO-S cells and investigated the antitumor activity in OSCC xenograft transplanted mice [25]. We have developed various anti-CD44v mAbs, including $C_{44}$Mab-6 (anti-CD44v3 mAb) [26], $C_{44}$Mab-108 (anti-CD44v4 mAb) [27], $C_{44}$Mab-3 (anti-CD44v5 mAb) [28], $C_{44}$Mab-9 (anti-CD44v6 mAb) [29], $C_{44}$Mab-34 (anti-CD44v7/8 mAb) [30], and $C_{44}$Mab-1 (anti-CD44v9 mAb) [31].

In this study, we established a novel anti-CD44v10 mAb, $C_{44}$Mab-18 (IgM, kappa) by CBIS method, and evaluated its applications, including flow cytometry, western blotting, and immunohistochemical analyses of OSCC tissues.

## 2. Materials and Methods

### *2.1. Cell Lines*

A mouse multiple myeloma P3X63Ag8U.1 (P3U1) and Chinese hamster ovary (CHO)-K1 cell lines were obtained from the American Type Culture Collection (ATCC, Manassas, VA, USA). The human pancreatic cancer cell line (PANC-1) was obtained from the Cell Resource Center for Biomedical Research Institute of Development, Aging, and Cancer at Tohoku University (Sendai, Japan). To culture these cell lines, we used RPMI-1640 medium (Nacalai Tesque, Inc., Kyoto, Japan), which is supplemented with 10% heat-inactivated fetal bovine serum (FBS; Thermo Fisher Scientific, Inc., Waltham, MA, USA). The antibiotics, including 100 μg/mL streptomycin, 100 U/mL penicillin, and 0.25 μg/mL amphotericin B (Nacalai Tesque, Inc.) were added to the media. A human OSCC cell line, HSC-3 was obtained from the Japanese Collection of Research Bioresources (Osaka, Japan), and cultured in DMEM medium (Nacalai Tesque, Inc., Kyoto, Japan), supplemented as indicated above. All cell lines were grown in a humidified incubator at 37°C with 5% $CO_2$.

The cDNAs of CD44v3–10 and CD44s were obtained as described previously [20]. The cDNAs were cloned into pCAG-zeo-ssPA16 and pCAG-neo-ssPA16 vectors with a signal sequence and N-terminal PA16 tag (GLEGGVAMPGAEDDVV) [20,32-35]. The PA16 tag can be detected by NZ-1 mAb, which was originally developed as an anti-human podoplanin (PDPN) mAb [36-48]. Using a Neon transfection system (Thermo Fisher Scientific, Inc.), stable transfectants, such as PANC-1/CD44v3–10, CHO/CD44v3–10, and CHO/CD44s, were established by introducing corresponding vectors into the cells.

### *2.2. Production of hybridoma cells*

PANC-1/CD44v3–10 ($1 \times 10^8$ cells) was intraperitoneally administrated into the 6-week-old female BALB/c mice (CLEA Japan, Tokyo, Japan) with Imject Alum (Thermo Fisher Scientific Inc.). Additional three times immunizations of PANC-1/CD44v3–10 ($1 \times 10^8$ cells) and a booster injection of PANC-1/CD44v3–10 ($1 \times 10^8$ cells) two days before the sacrifice was performed. Hybridomas were produced as described previously [28]. The supernatants were selected by flow cytometer (SA3800 Cell Analyzer) and SA3800 software (ver. 2.05, Sony Corp. Tokyo, Japan).

### *2.3. Enzyme–linked immunosorbent assay (ELISA)*

Thirty-four peptides, which cover the variant region of CD44v3–10 [22], were obtained from Sigma-Aldrich Corp. (St. Louis, MO, USA), and immobilized on Nunc Maxisorp 96-well immunoplates (Thermo Fisher Scientific Inc) at 20 μg/mL. After the blocking with 1% (*w*/*v*) bovine serum albumin (BSA) in phosphate-buffered saline (PBS) containing 0.05% (*v*/*v*) Tween 20 (PBST; Nacalai Tesque, Inc.), $C_{44}$Mab-18 (1 μg/mL) was added to each well. Then, the wells were further treated with anti-mouse immunoglobulins peroxidase-conjugate (1:2000 diluted; Agilent Technologies Inc., Santa Clara, CA, USA). The ELISA POD Substrate TMB Kit (Nacalai Tesque, Inc.) was used for enzymatic reactions. Using an iMark microplate reader (Bio-Rad Laboratories, Inc., Berkeley, CA, USA), the optical density (655 nm) was measured.

### *2.4. Flow Cytometry*

HSC-3, CHO/CD44v3–10, and CHO-K1 cells ($1 \times 10^5$ cells/sample) were incubated with $C_{44}$Mab-18, $C_{44}$Mab-46, or blocking buffer (0.1% BSA in PBS; control) for 30 min at 4°C. Then, the cells were treated with anti-mouse IgG conjugated with Alexa Fluor 488 (1:2000; Cell Signaling Technology, Inc.) for 30 min at 4°C. Fluorescence data were collected and analyzed as indicated above.

### *2.5. Determination of Apparent Dissociation Constant ($K_D$) by Flow Cytometry*

The serially diluted $C_{44}$Mab-18 at the indicated concentrations was suspended with $2 \times 10^5$ of HSC-3 and CHO/CD44v3–10 cells. Then, the cells were treated with anti-mouse IgG conjugated with Alexa Fluor 488 (1:200). Fluorescence data were analyzed, and the apparent dissociation constant ($K_D$) was determined by the fitting binding isotherms to

built-in one-site binding models of GraphPad Prism 8 (GraphPad Software, Inc., La Jolla, CA, USA).

### *2.6. Western Blot Analysis*

The 10 μg of cell lysates were subjected to SDS-polyacrylamide gel for electrophoresis using polyacrylamide gels (5–20%; FUJIFILM Wako Pure Chemical Corporation, Osaka, Japan) and electrotransferred onto polyvinylidene difluoride membranes (Merck KGaA, Darmstadt, Germany). After the blocking using 4% skim milk (Nacalai Tesque, Inc.) in PBST, the membranes were incubated with 10 μg/mL of $C_{44}$Mab-18, 10 μg/mL of $C_{44}$Mab-46, or 0.5 μg/mL of an anti-β-actin mAb (clone AC-15; Sigma-Aldrich Corp.). The membranes were further treated with peroxidase-conjugated anti-mouse immunoglobulins (diluted 1:1000; Agilent Technologies, Inc.). Finally, the chemiluminescence signal was obtained using ImmunoStar LD (FUJIFILM Wako Pure Chemical Corporation) and was detected by a Sayaca-Imager (DRC Co. Ltd., Tokyo, Japan).

### *2.7. Immunohistochemical Analysis*

Formalin-fixed paraffin-embedded (FFPE) sections of OSCC tissue array (OR601c; US Biomax Inc., Rockville, MD, USA) were autoclaved in EnVision FLEX Target Retrieval Solution High pH (Agilent Technologies, Inc.). After blocking with SuperBlock T20 (Thermo Fisher Scientific, Inc.), the sections were incubated with $C_{44}$Mab-18 (1 μg/mL) and $C_{44}$Mab-46 (1 μg/mL) for 1 h at room temperature. The sections were further treated with the EnVision+ Kit for a mouse (Agilent Technologies Inc.) for 30 min at room temperature. The chromogenic reaction and counterstaining were performed using 3,3′-diaminobenzidine tetrahydrochloride (DAB; Agilent Technologies Inc.) and hematoxylin (FUJIFILM Wako Pure Chemical Corporation), respectively.

## 3. Results

### *3.1. Establishment of an Anti-CD44 mAbs by immunization of PANC-1/CD44v3–10 cells*

We have established anti-CD44 mAbs, including $C_{44}$Mab-5 (pan-CD44) [20], $C_{44}$Mab-6 (v3) [26], $C_{44}$Mab-3 (v5) [28], $C_{44}$Mab-9 (v6) [29], and $C_{44}$Mab-1 (v9) [31] using CHO/CD44v3–10 cells as an immunogen. In this study, we established another stable transfectant (PANC-1/CD44v3–10 cells) (Figure 1A). Mice were immunized with PANC-1/CD44v3–10 cells (Figure 1B), and hybridomas were produced by fusion between the splenocyte and P3U1 cells (Figure 1C). Then, the supernatants, which were reactive to CHO/CD44v3–10 cells, but not to CHO-K1, were selected by flow cytometry-based high throughput screening (Figure 1D). After cloning, anti-CD44 mAb-producing clones were finally established (Figure 1E).

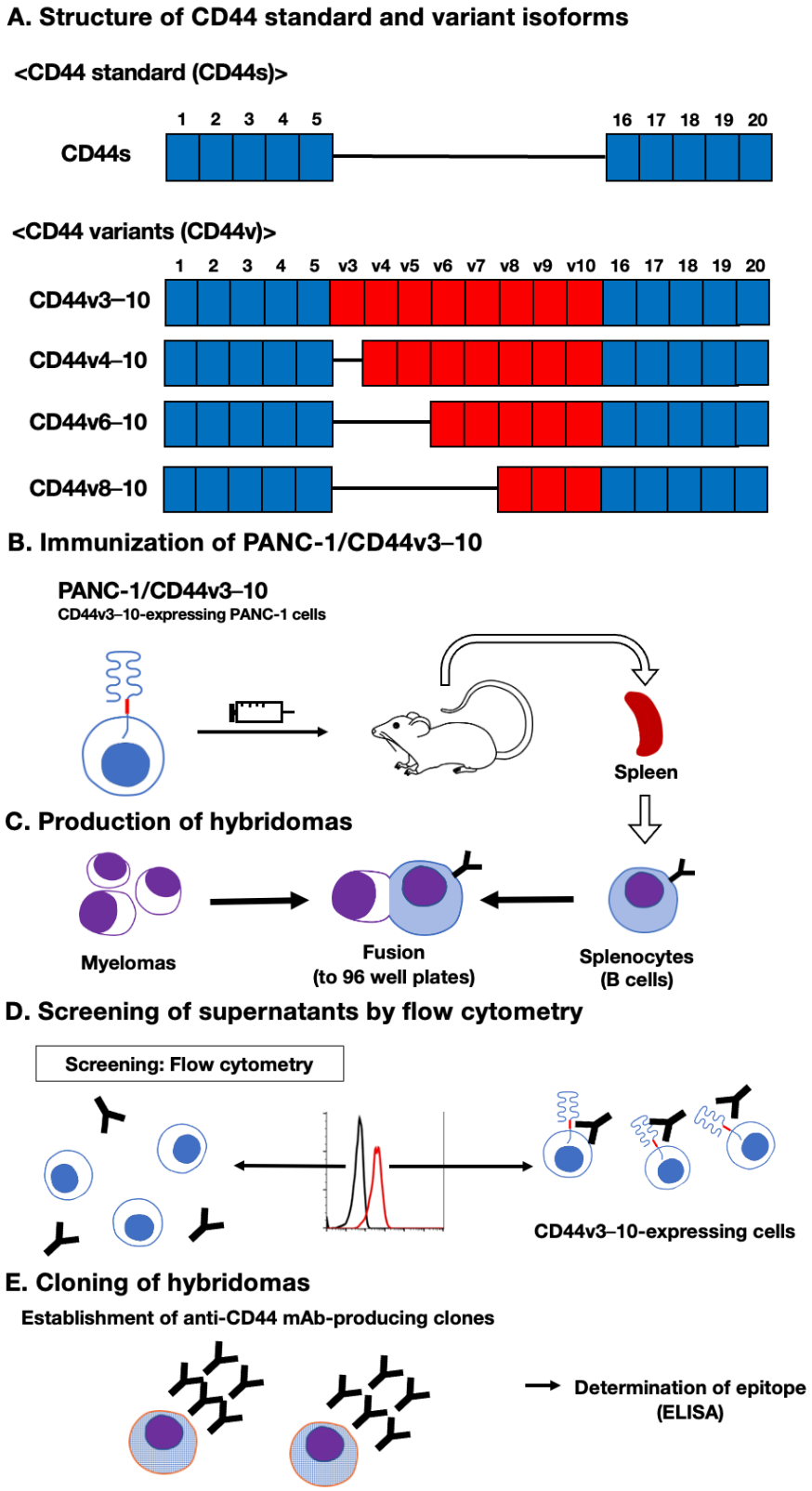


**Figure 1.** A schematic illustration of the CBIS method to establish ant-human CD44 mAbs. (**A**) Structure of CD44. The CD44s mRNA contains the constant exons (1 to 5) and (16 to 20). The CD44v mRNAs are produced by the alternative splicing of variant exons such as CD44v3–10, CD44v4–10, CD44v6–10, and CD44v8–10. (**B**) PANC-1/CD44v3–10 cells were intraperitoneally injected into BALB/c mice. (**C**) Hybridomas were produced by the fusion of the splenocytes and P3U1 cells (**D**) The screening was performed by flow cytometry using CHO/CD44v3–10 and parental CHO-K1 cells. (**E**) After cloning and additional screening, a clone C44Mab-18 (IgM, kappa) was established.

### *3.2. Flow Cytometric Analysis of C44Mab-18 to CD44-Expressing Cells*

In this study, established clones, the epitope of which includes CD44v10, were mainly determined to be IgM although all mAbs against other CD44 variants are IgG [26-31]. Among those clones, we examined the reactivity of C44Mab-18 (IgM, kappa) against CHO/CD44v3–10 and CHO/CD44s cells by flow cytometry. C44Mab-18 dose-dependently recognized CHO/CD44v3–10 cells (Figure 2A). In contrast, C44Mab-18 neither recognized CHO/CD44s (Figure 2B) nor CHO-K1 (Figure 2C) cells. We confirmed that an anti-pan-CD44 mAb, C44Mab-46 [21], recognized CHO/CD44s cells, but not CHO-K1 cells (Supplementary Figure S1). Furthermore, C44Mab-18 could recognize HSC-3 cells (Figure 2D) in a dose-dependent manner. These results indicated that C44Mab-18 recognizes the variant exon-encoded region between v3 and v10 (Figure 1A).

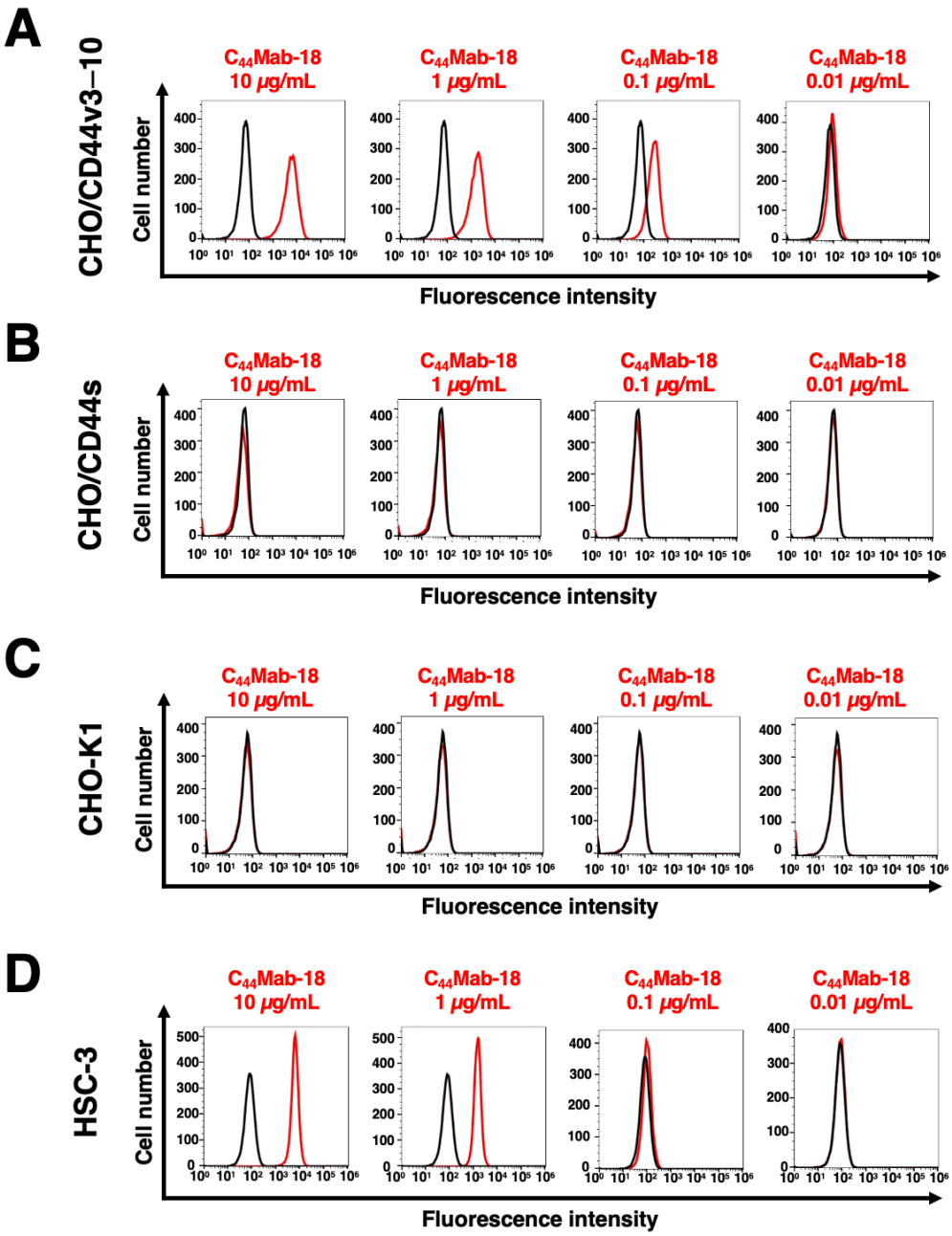


**Figure 2.** Flow cytometry using C44Mab-18. CHO/CD44v3–10 (**A**), CHO/CD44s (**B**), CHO-K1 (**C**), and HSC-3 (**D**) cells were treated with 0.01–10 μg/mL of C44Mab-18. Then, cells were treated with Alexa Fluor 488-conjugated anti-mouse IgG (Red line). The black line represents the negative control (blocking buffer).

### *3.3. Epitope Mapping of C44Mab-18 by ELISA*

To determine the epitope of C44Mab-18, we performed the ELISA using synthetic peptides, which cover the variant exon-encoded region between v3 and v10 [22]. As shown in Figure 3, C44Mab-18 recognized the CD44 p551–570 peptide (SNSNVNRSLSGDQDTFHPSG), which is corresponding to variant 10 and constant exon 16-encoded sequence (Supplementary Table S1). In contrast, C44Mab-18 never recognized other v3 and v10-encoded peptides. This and Figure 2 results indicated that C44Mab-18 specifically recognizes the variant 10-containing CD44.

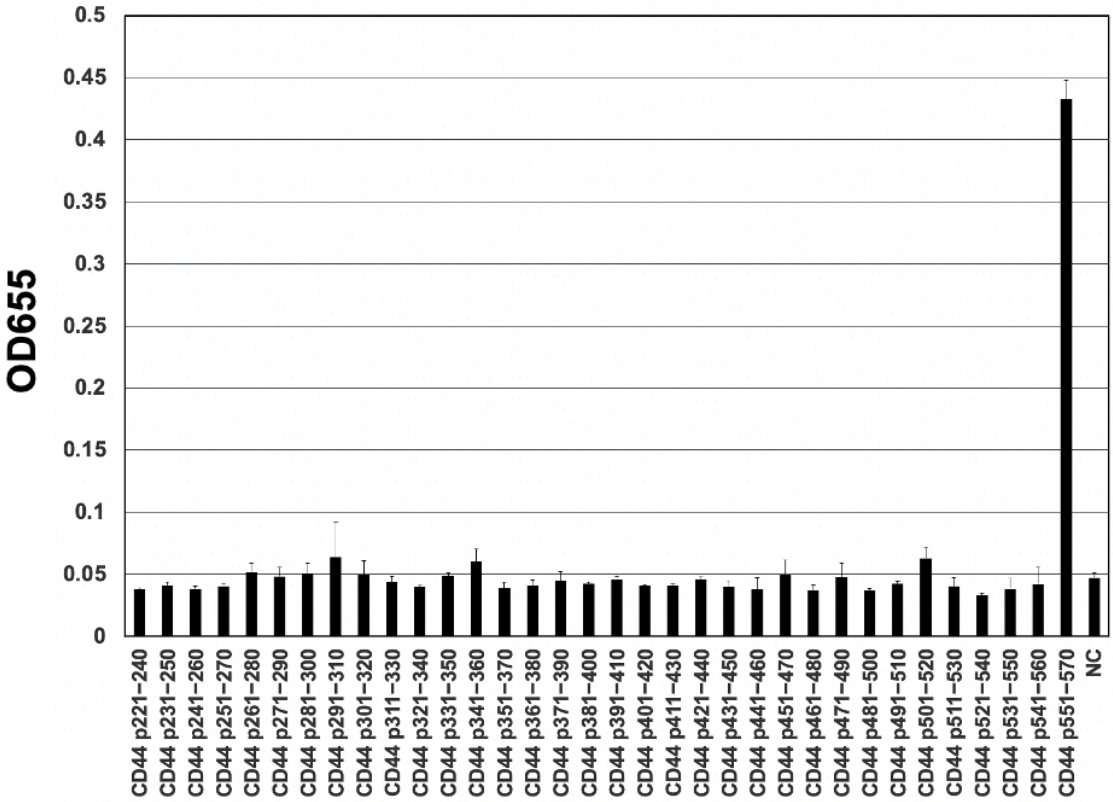


**Figure 3.** Determination of C44Mab-18 epitope by ELISA. The synthesized peptides, which cover the variant exon-encoded region between v3 and v10, were immobilized on immunoplates. The plates were incubated with C44Mab-18, followed by incubation with peroxidase-conjugated anti-mouse immunoglobulins. Optical density was measured at 655 nm. The CD44 p551–570 sequence (SNSNVNRSLSGDQDTFHPSG) is corresponding to variant 10 and the constant exon 16-encoded sequence. Error bars represent means ± SDs. NC, negative control (0.1% DMSO [solvent] in PBS).

### *3.3. Determination of the apparent Binding Affinity of C44Mab-18 by Flow Cytometry*

We next measured the apparent binding affinity of C44Mab-18 to CHO/CD44v3–10 and HSC-3 cells using flow cytometry. The dissociation constant ($K_D$) of C44Mab-18 for CHO/CD44v3–10 (Figure 4A) and HSC-3 (Figure 4B) were $1.6 \times 10^{-7}$ M and $1.7 \times 10^{-7}$ M, respectively. These results indicated that C44Mab-18 possesses a moderate binding affinity for CD44v3–10 or endogenous CD44v10-expressing cells.

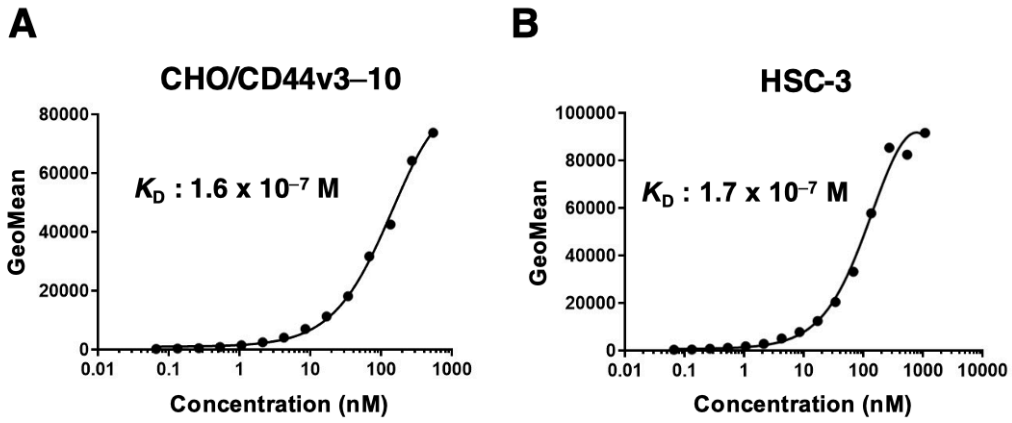


**Figure 4.** The determination of the binding affinity of C44Mab-18. C44Mab-18 at indicated concentrations was treated with CHO/CD44v3–10 (**A**) and HSC-3 (**B**). Then, cells were treated with anti-mouse IgG conjugated with Alexa Fluor 488. Fluorescence data were collected, followed by the calculation of the apparent dissociation constant ($K_D$) by GraphPad PRISM 8.

### *3.4. Western Blot Analysis*

To assess the sensitivity of C44Mab-18 in western blot analysis, we prepared the cell lysates of CHO-K1, CHO/CD44s, and CHO/CD44v3–10. C44Mab-18 mainly detected CD44v3–10 as more than 180-kDa and ~70-kDa bands. However, C44Mab-18 did not detect any bands from lysates of CHO/CD44s and CHO-K1 cells (Figure 5A). An anti-pan-CD44 mAb, C44Mab-46, recognized both CD44s (~75 kDa) and CD44v3–10 (>180 kDa) bands in the lysates of CHO/CD44s and CHO/CD44v3–10, respectively (Figure 5B). We used β-actin as a loading control (Figure 5C). These results indicated that C44Mab-18 can detect exogenous CD44v3–10.

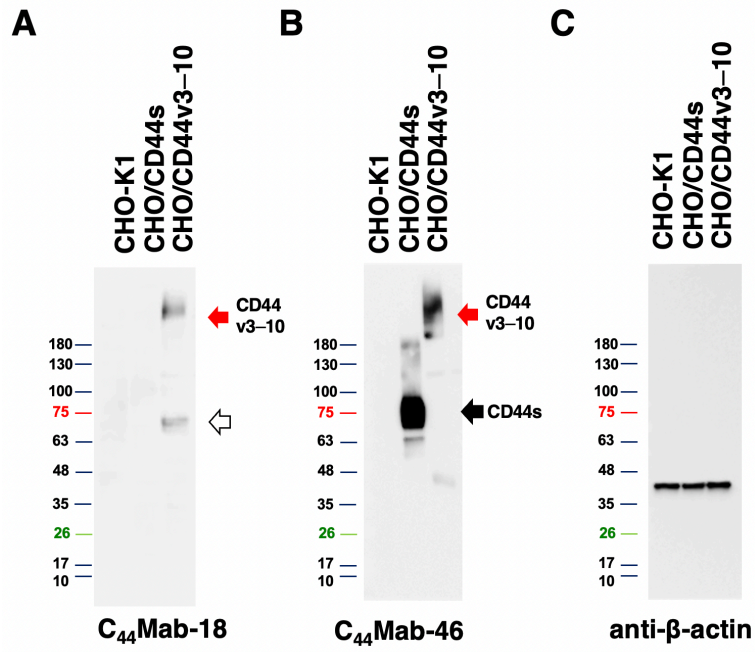


**Figure 5.** Western blot analysis by C44Mab-18. The total cell lysates (10 μg of protein) were separated and transferred onto polyvinylidene difluoride (PVDF) membranes. The membranes were incubated with 10 μg/mL of C44Mab-18 (**A**), 10 μg/mL of C44Mab-46 (**B**), or 0.5 μg/mL of an anti-β-actin mAb (**C**), followed by incubation with peroxidase-conjugated anti-mouse immunoglobulins. The red arrows indicate the CD44v3–10 (>180 kDa). The black arrow indicates the CD44s (~75 kDa). The white arrow indicates a lower molecular weight band recognized by C44Mab-18 in CHO/CD44v3–10 lysate (~70 kDa).

### *3.5. Immunohistochemical Analysis using C44Mab-18 against Tumor Tissues*

Since HNSCC is revealed as the second highest CD44-expressing cancer type in the Pan-Cancer Atlas [5], we examined the reactivity of C44Mab-18 and C44Mab-46 in immunohistochemical analyses using FFPE sections of OSCC tissue array. As shown in Figure 6, C44Mab-18 exhibited membranous staining and was able to distinguish tumor cells from stromal tissues. In contrast, C44Mab-46 stained both. We summarized the data of immunohistochemical analyses in Table 1; C44Mab-18 stained 41 out of 50 cases (82%) in OSCC. These results indicated that C44Mab-18 applies to immunohistochemical analysis of FFPE tumor sections.

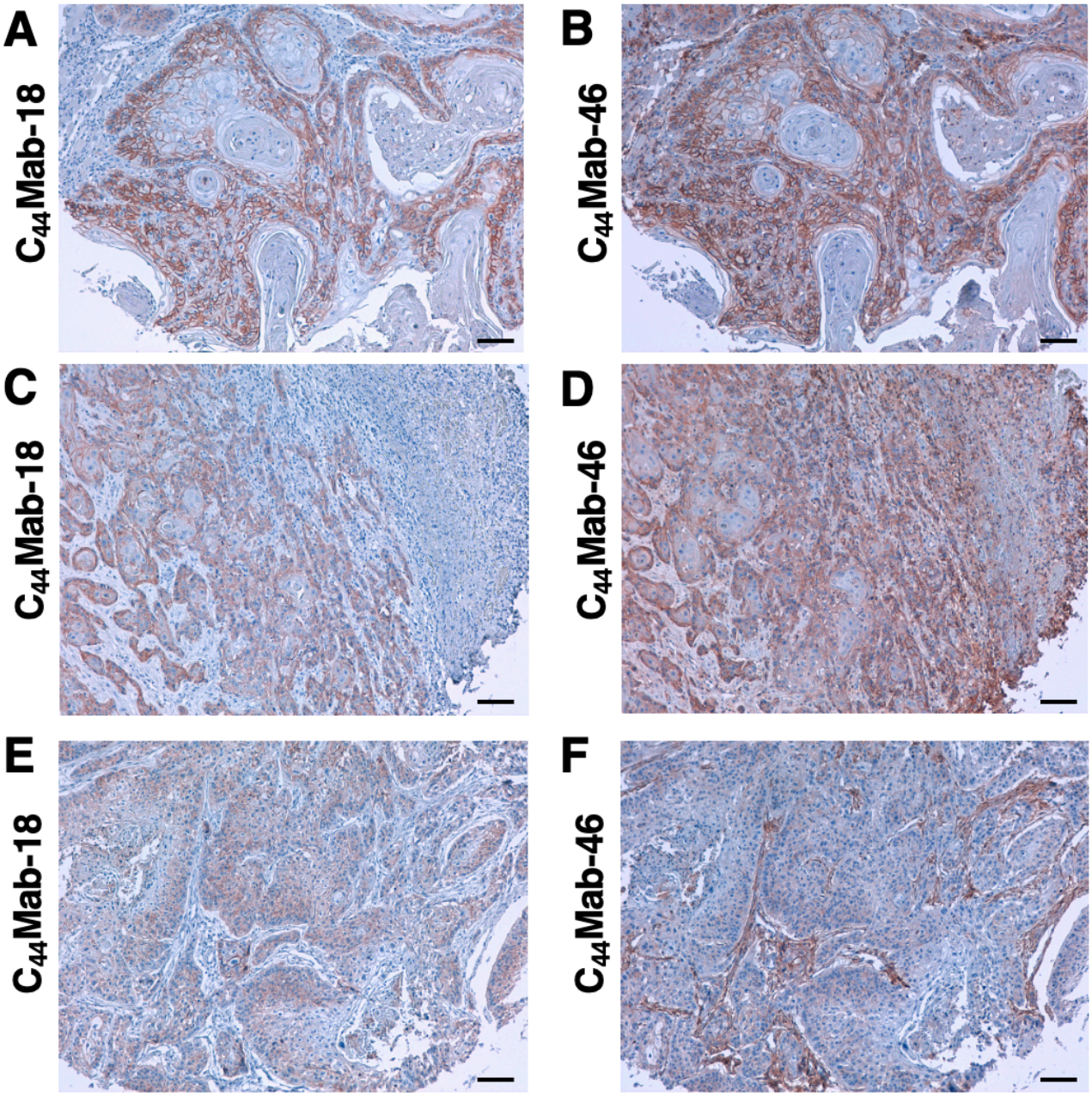


**Figure 6.** Immunohistochemical analysis using C44Mab-18 and C44Mab-46 against OSCC tissues. (**A**–**F**) Serial sections of the OSCC tissue array (OR601c) were incubated with 1 μg/mL of C44Mab-18 or C44Mab-46 followed by treatment with the Envision+ kit. The color was developed using 3,3′-diaminobenzidine tetrahydrochloride (DAB), and the sections were counterstained with hematoxylin. Scale bar = 100 μm.

**Table 1.** Immunohistochemical analysis using $C_{44}$Mab-18 against OSCC tissue array.

| No. | Age | Sex | Organ /Anatomic Site | Pathology diagnosis | TNM | $C_{44}$Mab-18 | $C_{44}$Mab-46 |
|---|---|---|---|---|---|---|---|
| 1 | 78 | M | Tongue | SCC of tongue | T2N0M0 | + | + |
| 2 | 40 | M | Tongue | SCC of tongue | T2N0M0 | + | ++ |
| 3 | 75 | F | Tongue | SCC of tongue | T2N0M0 | - | + |
| 4 | 35 | F | Tongue | SCC of tongue | T2N0M0 | ++ | ++ |
| 5 | 61 | M | Tongue | SCC of tongue | T2N0M0 | ++ | +++ |
| 6 | 41 | F | Tongue | SCC of tongue | T2N0M0 | + | + |
| 7 | 64 | M | Tongue | SCC of right tongue | T2N2M0 | ++ | ++ |
| 8 | 76 | M | Tongue | SCC of tongue | T1N0M0 | ++ | ++ |
| 9 | 50 | F | Tongue | SCC of tongue | T2N0M0 | ++ | ++ |
| 10 | 44 | M | Tongue | SCC of tongue | T2N1M0 | ++ | +++ |
| 11 | 53 | F | Tongue | SCC of tongue | T1N0M0 | + | ++ |
| 12 | 46 | F | Tongue | SCC of tongue | T2N0M0 | ++ | + |
| 13 | 50 | M | Tongue | SCC of root of tongue | T3N1M0 | ++ | + |
| 14 | 36 | F | Tongue | SCC of tongue | T1N0M0 | ++ | +++ |
| 15 | 63 | F | Tongue | SCC of tongue | T1N0M0 | + | + |
| 16 | 46 | M | Tongue | SCC of tongue | T2N0M0 | + | - |
| 17 | 58 | M | Tongue | SCC of tongue | T2N0M0 | + | + |
| 18 | 64 | M | Lip | SCC of lower lip | T1N0M0 | + | +++ |
| 19 | 57 | M | Lip | SCC of lower lip | T2N0M0 | + | +++ |
| 20 | 61 | M | Lip | SCC of lower lip | T1N0M0 | + | ++ |
| 21 | 60 | M | Gum | SCC of gum | T3N0M0 | ++ | + |
| 22 | 60 | M | Gum | SCC of gum | T1N0M0 | +++ | +++ |
| 23 | 69 | M | Gum | SCC of upper gum | T3N0M0 | ++ | ++ |
| 24 | 53 | M | Bucca cavioris | SCC of bucca cavioris | T2N0M0 | ++ | + |
| 25 | 55 | M | Bucca cavioris | SCC of bucca cavioris | T1N0M0 | +++ | + |
| 26 | 58 | M | Tongue | SCC of base of tongue | T1N0M0 | ++ | ++ |
| 27 | 63 | M | Oral cavity | SCC | T1N0M0 | +++ | ++ |
| 28 | 48 | F | Tongue | SCC of tongue | T1N0M0 | + | + |
| 29 | 80 | M | Lip | SCC of lower lip | T1N0M0 | +++ | +++ |
| 30 | 77 | M | Tongue | SCC of base of tongue | T2N0M0 | ++ | ++ |
| 31 | 59 | M | Tongue | SCC of tongue | T2N0M0 | + | - |
| 32 | 77 | F | Tongue | SCC of tongue | T1N0M0 | + | ++ |
| 33 | 56 | M | Tongue | SCC of root of tongue | T2N1M0 | + | + |
| 34 | 60 | M | Tongue | SCC of tongue | T2N1M0 | ++ | ++ |
| 35 | 62 | M | Tongue | SCC of tongue | T2N0M0 | + | ++ |
| 36 | 67 | F | Tongue | SCC of tongue | T2N0M0 | - | ++ |
| 37 | 47 | F | Tongue | SCC of tongue | T2N0M0 | +++ | +++ |
| 38 | 37 | M | Tongue | SCC of tongue | T2N1M0 | - | - |

| | | | | | | | |
|---|---|---|---|---|---|---|---|
| 39 | 55 | F | Tongue | SCC of tongue | T2N0M0 | + | + |
| 40 | 56 | F | Bucca cavioris | SCC of bucca cavioris | T2N0M0 | + | + |
| 41 | 49 | M | Bucca cavioris | SCC of bucca cavioris | T1N0M0 | - | - |
| 42 | 45 | M | Bucca cavioris | SCC of bucca cavioris | T2N0M0 | - | - |
| 43 | 42 | M | Bucca cavioris | SCC of bucca cavioris | T3N0M0 | +++ | ++ |
| 44 | 44 | M | Jaw | SCC of right drop jaw | T1N0M0 | + | +++ |
| 45 | 40 | F | Tongue | SCC of base of tongue | T2N0M0 | - | ++ |
| 46 | 49 | M | Bucca cavioris | SCC of bucca cavioris | T1N0M0 | ++ | +++ |
| 47 | 56 | F | Tongue | SCC of base of tongue | T2N0M0 | - | + |
| 48 | 42 | M | Bucca cavioris | SCC a of bucca cavioris | T3N0M0 | +++ | +++ |
| 49 | 87 | F | Face | SCC a of left face | T2N0M0 | - | + |
| 50 | 50 | M | Gum | SCC of gum | T2N0M0 | - | - |

-, No stain; +, Weak intensity; ++, Moderate intensity; +++, Strong intensity.

## 4. Discussion

We have established anti-CD44 mAbs using CHO/CD44v3–10 [20,26,28,29,31], purified CD44v3–10 ectodomain [21,30], or PANC-1/CD44v3–10 (this study) as antigens. We prepared the list of them in "Antibody Bank" (see Supplementary Materials). In this study, we listed a novel anti-CD44v antibody $C_{44}$Mab-18, which recognizes the border sequence between variant 10 and constant exon 16 (Figure 3). Furthermore, $C_{44}$Mab-18 could recognize CHO/CD44v3–10, but not CHO/CD44s in flow cytometry (Figure 2) and western blot analyses (Figure 5). Moreover, $C_{44}$Mab-18 could stain tumor cells, but not stromal tissues, which could be stained by $C_{44}$Mab-46, an anti-pan-CD44 mAb (Figure 6). These results indicate that $C_{44}$Mab-18 is an anti-CD44v10 mAb.

The VFF series anti-human CD44v mAbs were previously established by the immunization of glutathione *S*-transferase fused CD44v3–10 produced by bacteria [49,50]. The clones, VFF-8 (anti-CD44v5), VFF-18 (anti-CD44v6), VFF-9 (anti-CD44v7), VFF-17 (anti-CD44v7/8), and VFF-14 (anti-CD44v10) have been used for various applications [51]. Although VFF14 was shown to apply to immunohistochemistry [52], the detailed binding epitope of VFF-14 has not been reported. In this study, we determined the epitope of $C_{44}$Mab-18 as the CD44 p551–570 peptide (<u>SNSNVNRSLSG</u>DQDTFHPSG), which is corresponding to variant 10 (underlined) and constant exon 16-encoded region. In contrast, $C_{44}$Mab-18 never recognizes the p541–560 peptide (FGVTAVTVGDSNSNVNRSLS) in the variant 10 region. Therefore, $C_{44}$Mab-18 could have the epitope in the border region, but the inclusion of variant 10 is essential for the recognition.

Since the CD44 protein is modified by a variety of *N*-glycans and *O*-glycans, the molecular weight of CD44v isoforms surpasses 200 kDa [53]. $C_{44}$Mab-18 recognized both more than 180-kDa and ~70-kDa bands (Figure 5A) in the lysate from CHO/CD44v3–10. The 70 kDa is approximately identical to the predicted molecular weight of CD44v3–10 from the amino acid sequence. Therefore, $C_{44}$Mab-18 could recognize CD44v3–10 regardless of the glycosylation. The detailed epitope mapping and the influence of glycosylation on $C_{44}$Mab-18 recognition should be investigated in future studies.

CD44v8–10 was shown to interact with xCT, a glutamate-cystine transporter, and regulate the level of reduced glutathione in tumor cells. The interaction is important for the stabilization of xCT on the cell surface, which promotes the defense against reactive oxygen species [17]. Furthermore, the interaction failed in CD44v8–10 (S301A), an *N*-linked glycosylation consensus motif (Asn-X-Ser/Thr) mutant in the variant 10-encoded region [17]. Therefore, it is worthwhile to investigate whether $C_{44}$Mab-18 interferes with the interaction between CD44v8–10 and xCT in future studies. Furthermore, several studies revealed that CD44v9 is used as a predictive marker for recurrence [54] and a

biomarker for patient selection and efficacy of xCT inhibitors, sulfasalazine in gastric cancer [55]. Further investigations are also required to clarify the clinical significance of CD44v10 expression using $C_{44}$Mab-94.

The mAbs against CD44 have been considered a therapeutic option for solid tumors and leukemia [12]. However, anti-pan-CD44 mAbs can affect normal tissues such as epithelium and hematopoiesis. In a preclinical study using a murine thymoma model, a comparative study between an anti-pan-CD44 mAb (IM-7) and an anti-murine CD44v10 mAb (K926) was conducted in CD44v10 transfected EL4 thymoma (EL4-v10) [56]. The results showed that a blockade of CD44v10 by K926 was superior to that of IM-7 in intra-marrow EL4-v10 growth retardation. Furthermore, K926 hardly disturbed the hematopoietic stem cell (HSC) interaction with the bone marrow stroma. In contrast, IM-7 strongly affected the embedding of HSC in the bone marrow stroma [56]. These results indicated that the therapeutic use of anti-pan-CD44 mAbs should be avoided in favor of CD44v-specific mAbs as far as leukemic cells express CD44v isoforms.

In a humanized mouse model, CD44v8–10 was elevated during chronic myeloid leukemia progression from chronic phase to blast crisis [57]. Furthermore, increased transcription of CD44 mRNA was observed in human acute myeloid leukemia (AML) patients with *FLT3* or *DNMT3A* mutations through suppression of CpG islands methylation in the promoter [58]. An anti-CD44v6 mAb (BIWA-8) derived from VFF-18 [59] was engineered to develop chimeric antigen receptors (CARs) for AML with *FLT3* or *DNMT3A* mutations. The CD44v6 CAR-T cells exhibited potent anti-leukemic effects [58]. We have established class-switched and defucosylated $IgG_{2a}$ recombinant mAbs and evaluated the antitumor activity in xenograft models [25,60-66]. Therefore, the production of class-switched and defucosylated $C_{44}$Mab-18 is one of the important strategies to evaluate the antitumor effect in preclinical models.

Since anti-pan-CD44 and anti-CD44v mAbs still have the possibility of side effects by affecting normal tissues, the clinical applications are limited. This study used tumor cell-expressed CD44v3–10 as an immunogen. The strategy is critical for the development of cancer-specific mAbs (CasMabs). We developed podocalyxin-targeting CasMabs [67] and PDPN-targeting CasMabs [68-70], which react with the aberrantly glycosylated targets selectively expressed in cancer [71]. Anti-PDPN-CasMabs have been applied to CAR-T therapy in preclinical studies [72-74]. For CasMab development, we should perform a further selection of our established anti-CD44 mAbs by comparing the reactivity against normal cells and tissues. Anti-CD44 CasMabs could be applicable for designing the modalities, including antibody-drug conjugates and CAR-T.

**Supplementary Materials:** The following supporting information can be downloaded at: www.mdpi.com/xxx/s1. Supplementary Figure S1, Recognition of CHO/CD44s and CHO/CD44v3–10 by $C_{44}$Mab-46 by flow cytometry. Supplementary Table S1, The determination of the binding epitope of C44Mab-18 by ELISA.

The information on anti-CD44 mAbs in our laboratory is available in "Antibody Bank" [http://www.med-tohoku-antibody.com/topics/001_paper_antibody_PDIS.htm#CD44 (accessed on 20 May 2023)].

**Author Contributions:** K.I. and H.S. performed the experiments. M.K.K. and Y.K. designed the experiments. K.I. and H.S. analyzed the data. K.I., H.S., and Y.K. wrote the manuscript. All authors have read and agreed to the published version of the manuscript.

**Funding:** This research was supported in part by Japan Agency for Medical Research and Development (AMED) under Grant Numbers: JP23ama121008 (to Y.K.), JP23am0401013 (to Y.K.), and JP23ck0106730 (to Y.K.), and by the Japan Society for the Promotion of Science (JSPS) Grants-in-Aid for Scientific Research (KAKENHI) grant nos. 22K06995 (to H.S.), 21K07168 (to M.K.K.), and 22K07224 (to Y.K.).

**Institutional Review Board Statement:** The animal study protocol was approved by the Animal Care and Use Committee of Tohoku University (Permit number: 2019NiA-001) for studies involving animals.

**Informed Consent Statement:** Not applicable.

**Data Availability Statement:** All related data and methods are presented in this paper. Additional inquiries should be addressed to the corresponding authors.

**Conflicts of Interest:** The authors declare no conflicts of interest involving this article.

## References


1. Mody, M.D.; Rocco, J.W.; Yom, S.S.; Haddad, R.I.; Saba, N.F. Head and neck cancer. *Lancet* **2021**, *398*, 2289-2299, doi:10.1016/s0140-6736(21)01550-6.
2. Xing, D.T.; Khor, R.; Gan, H.; Wada, M.; Ermongkonchai, T.; Ng, S.P. Recent Research on Combination of Radiotherapy with Targeted Therapy or Immunotherapy in Head and Neck Squamous Cell Carcinoma: A Review for Radiation Oncologists. *Cancers (Basel)* **2021**, *13*, doi:10.3390/cancers13225716.
3. Muzaffar, J.; Bari, S.; Kirtane, K.; Chung, C.H. Recent Advances and Future Directions in Clinical Management of Head and Neck Squamous Cell Carcinoma. *Cancers (Basel)* **2021**, *13*, doi:10.3390/cancers13020338.
4. Johnson, D.E.; Burtness, B.; Leemans, C.R.; Lui, V.W.Y.; Bauman, J.E.; Grandis, J.R. Head and neck squamous cell carcinoma. *Nat Rev Dis Primers* **2020**, *6*, 92, doi:10.1038/s41572-020-00224-3.
5. Ludwig, N.; Szczepanski, M.J.; Gluszko, A.; Szafarowski, T.; Azambuja, J.H.; Dolg, L.; Gellrich, N.C.; Kampmann, A.; Whiteside, T.L.; Zimmerer, R.M. CD44(+) tumor cells promote early angiogenesis in head and neck squamous cell carcinoma. *Cancer Lett* **2019**, *467*, 85-95, doi:10.1016/j.canlet.2019.10.010.
6. Ponta, H.; Sherman, L.; Herrlich, P.A. CD44: from adhesion molecules to signalling regulators. *Nat Rev Mol Cell Biol* **2003**, *4*, 33-45, doi:10.1038/nrm1004.
7. Chen, C.; Zhao, S.; Karnad, A.; Freeman, J.W. The biology and role of CD44 in cancer progression: therapeutic implications. *J Hematol Oncol* **2018**, *11*, 64, doi:10.1186/s13045-018-0605-5.
8. Slevin, M.; Krupinski, J.; Gaffney, J.; Matou, S.; West, D.; Delisser, H.; Savani, R.C.; Kumar, S. Hyaluronan-mediated angiogenesis in vascular disease: uncovering RHAMM and CD44 receptor signaling pathways. *Matrix Biol* **2007**, *26*, 58-68, doi:10.1016/j.matbio.2006.08.261.
9. Valastyan, S.; Weinberg, R.A. Tumor metastasis: molecular insights and evolving paradigms. *Cell* **2011**, *147*, 275-292, doi:10.1016/j.cell.2011.09.024.
10. de Visser, K.E.; Joyce, J.A. The evolving tumor microenvironment: From cancer initiation to metastatic outgrowth. *Cancer Cell* **2023**, *41*, 374-403, doi:10.1016/j.ccell.2023.02.016.
11. Zöller, M. CD44, Hyaluronan, the Hematopoietic Stem Cell, and Leukemia-Initiating Cells. *Front Immunol* **2015**, *6*, 235, doi:10.3389/fimmu.2015.00235.
12. Hassn Mesrati, M.; Syafruddin, S.E.; Mohtar, M.A.; Syahir, A. CD44: A Multifunctional Mediator of Cancer Progression. *Biomolecules* **2021**, *11*, doi:10.3390/biom11121850.
13. Zöller, M. CD44: can a cancer-initiating cell profit from an abundantly expressed molecule? *Nat Rev Cancer* **2011**, *11*, 254-267, doi:10.1038/nrc3023.
14. Prince, M.E.; Sivanandan, R.; Kaczorowski, A.; Wolf, G.T.; Kaplan, M.J.; Dalerba, P.; Weissman, I.L.; Clarke, M.F.; Ailles, L.E. Identification of a subpopulation of cells with cancer stem cell properties in head and neck squamous cell carcinoma. *Proc Natl Acad Sci U S A* **2007**, *104*, 973-978, doi:10.1073/pnas.0610117104.
15. Yang, J.; Antin, P.; Berx, G.; Blanpain, C.; Brabletz, T.; Bronner, M.; Campbell, K.; Cano, A.; Casanova, J.; Christofori, G., et al. Guidelines and definitions for research on epithelial-mesenchymal transition. *Nat Rev Mol Cell Biol* **2020**, *21*, 341-352, doi:10.1038/s41580-020-0237-9.
16. Davis, S.J.; Divi, V.; Owen, J.H.; Bradford, C.R.; Carey, T.E.; Papagerakis, S.; Prince, M.E. Metastatic potential of cancer stem cells in head and neck squamous cell carcinoma. *Arch Otolaryngol Head Neck Surg* **2010**, *136*, 1260-1266, doi:10.1001/archoto.2010.219.
17. Ishimoto, T.; Nagano, O.; Yae, T.; Tamada, M.; Motohara, T.; Oshima, H.; Oshima, M.; Ikeda, T.; Asaba, R.; Yagi, H., et al. CD44 variant regulates redox status in cancer cells by stabilizing the xCT subunit of system xc(-) and thereby promotes tumor growth. *Cancer Cell* **2011**, *19*, 387-400, doi:10.1016/j.ccr.2011.01.038.
18. Kagami, T.; Yamade, M.; Suzuki, T.; Uotani, T.; Tani, S.; Hamaya, Y.; Iwaizumi, M.; Osawa, S.; Sugimoto, K.; Baba, S., et al. High expression level of CD44v8-10 in cancer stem-like cells is associated with poor prognosis in esophageal squamous cell carcinoma patients treated with chemoradiotherapy. *Oncotarget* **2018**, *9*, 34876-34888, doi:10.18632/oncotarget.26172.
19. Hagiwara, M.; Kikuchi, E.; Tanaka, N.; Kosaka, T.; Mikami, S.; Saya, H.; Oya, M. Variant isoforms of CD44 involves acquisition of chemoresistance to cisplatin and has potential as a novel indicator for identifying a cisplatin-resistant population in urothelial cancer. *BMC Cancer* **2018**, *18*, 113, doi:10.1186/s12885-018-3988-3.
20. Yamada, S.; Itai, S.; Nakamura, T.; Yanaka, M.; Kaneko, M.K.; Kato, Y. Detection of high CD44 expression in oral cancers using the novel monoclonal antibody, C(44)Mab-5. *Biochem Biophys Rep* **2018**, *14*, 64-68, doi:10.1016/j.bbrep.2018.03.007.

21. Goto, N.; Suzuki, H.; Tanaka, T.; Asano, T.; Kaneko, M.K.; Kato, Y. Development of a Novel Anti-CD44 Monoclonal Antibody for Multiple Applications against Esophageal Squamous Cell Carcinomas. *Int J Mol Sci* **2022**, *23*, doi:10.3390/ijms23105535.
22. Takei, J.; Asano, T.; Suzuki, H.; Kaneko, M.K.; Kato, Y. Epitope Mapping of the Anti-CD44 Monoclonal Antibody (C44Mab-46) Using Alanine-Scanning Mutagenesis and Surface Plasmon Resonance. *Monoclon Antib Immunodiagn Immunother* **2021**, *40*, 219-226, doi:10.1089/mab.2021.0028.
23. Asano, T.; Kaneko, M.K.; Takei, J.; Tateyama, N.; Kato, Y. Epitope Mapping of the Anti-CD44 Monoclonal Antibody (C44Mab-46) Using the REMAP Method. *Monoclon Antib Immunodiagn Immunother* **2021**, *40*, 156-161, doi:10.1089/mab.2021.0012.
24. Asano, T.; Kaneko, M.K.; Kato, Y. Development of a Novel Epitope Mapping System: RIEDL Insertion for Epitope Mapping Method. *Monoclon Antib Immunodiagn Immunother* **2021**, *40*, 162-167, doi:10.1089/mab.2021.0023.
25. Takei, J.; Kaneko, M.K.; Ohishi, T.; Hosono, H.; Nakamura, T.; Yanaka, M.; Sano, M.; Asano, T.; Sayama, Y.; Kawada, M., et al. A defucosylated antiCD44 monoclonal antibody 5mG2af exerts antitumor effects in mouse xenograft models of oral squamous cell carcinoma. *Oncol Rep* **2020**, *44*, 1949-1960, doi:10.3892/or.2020.7735.
26. Suzuki, H.; Kitamura, K.; Goto, N.; Ishikawa, K.; Ouchida, T.; Tanaka, T.; Kaneko, M.K.; Kato, Y. A Novel Anti-CD44 Variant 3 Monoclonal Antibody C(44)Mab-6 Was Established for Multiple Applications. *Int J Mol Sci* **2023**, *24*, doi:10.3390/ijms24098411.
27. Suzuki, H.; Tanaka, T.; Goto, N.; Kaneko, M.K.; Kato, Y. Development of a Novel Anti-CD44 Variant 4 Monoclonal Antibody C44Mab-108 for Immunohistochemistry. *Curr Issues Mol Biol* **2023**, *45*, 1875-1888, doi:10.3390/cimb45030121.
28. Kudo, Y.; Suzuki, H.; Tanaka, T.; Kaneko, M.K.; Kato, Y. Development of a Novel Anti-CD44 variant 5 Monoclonal Antibody C44Mab-3 for Multiple Applications against Pancreatic Carcinomas. *Antibodies* **2023**, *12*, 31, doi:10.3390/antib12020031.
29. Ejima, R.; Suzuki, H.; Tanaka, T.; Asano, T.; Kaneko, M.K.; Kato, Y. Development of a Novel Anti-CD44 Variant 6 Monoclonal Antibody C(44)Mab-9 for Multiple Applications against Colorectal Carcinomas. *Int J Mol Sci* **2023**, *24*, doi:10.3390/ijms24044007.
30. Suzuki, H.; Ozawa, K.; Tanaka, T.; Kaneko, M.K.; Kato, Y. Development of a Novel Anti-CD44 Variant 7/8 Monoclonal Antibody, C44Mab-34, for Multiple Applications against Oral Carcinomas. *Biomedicines* **2023**, *11*, 1099, doi:10.3390/biomedicines11041099.
31. Tawara, M.; Suzuki, H.; Goto, N.; Tanaka, T.; Kaneko, M.K.; Kato, Y. A Novel Anti-CD44 Variant 9 Monoclonal Antibody C44Mab-1 was Developed for Immunohistochemical Analyses Against Colorectal Cancers *Curr. Issues Mol. Biol.* **2023**, *45*, 3658-3673, doi:10.3390/cimb45040238.
32. Kato, Y.; Yamada, S.; Furusawa, Y.; Itai, S.; Nakamura, T.; Yanaka, M.; Sano, M.; Harada, H.; Fukui, M.; Kaneko, M.K. PMab-213: A Monoclonal Antibody for Immunohistochemical Analysis Against Pig Podoplanin. *Monoclon Antib Immunodiagn Immunother* **2019**, *38*, 18-24, doi:10.1089/mab.2018.0048.
33. Furusawa, Y.; Yamada, S.; Itai, S.; Sano, M.; Nakamura, T.; Yanaka, M.; Fukui, M.; Harada, H.; Mizuno, T.; Sakai, Y., et al. PMab-210: A Monoclonal Antibody Against Pig Podoplanin. *Monoclon Antib Immunodiagn Immunother* **2019**, *38*, 30-36, doi:10.1089/mab.2018.0038.
34. Furusawa, Y.; Yamada, S.; Itai, S.; Nakamura, T.; Yanaka, M.; Sano, M.; Harada, H.; Fukui, M.; Kaneko, M.K.; Kato, Y. PMab-219: A monoclonal antibody for the immunohistochemical analysis of horse podoplanin. *Biochem Biophys Rep* **2019**, *18*, 100616, doi:10.1016/j.bbrep.2019.01.009.
35. Furusawa, Y.; Yamada, S.; Itai, S.; Nakamura, T.; Takei, J.; Sano, M.; Harada, H.; Fukui, M.; Kaneko, M.K.; Kato, Y. Establishment of a monoclonal antibody PMab-233 for immunohistochemical analysis against Tasmanian devil podoplanin. *Biochem Biophys Rep* **2019**, *18*, 100631, doi:10.1016/j.bbrep.2019.100631.
36. Kato, Y.; Kaneko, M.K.; Kuno, A.; Uchiyama, N.; Amano, K.; Chiba, Y.; Hasegawa, Y.; Hirabayashi, J.; Narimatsu, H.; Mishima, K., et al. Inhibition of tumor cell-induced platelet aggregation using a novel anti-podoplanin antibody reacting with its platelet-aggregation-stimulating domain. *Biochem Biophys Res Commun* **2006**, *349*, 1301-1307, doi:10.1016/j.bbrc.2006.08.171.
37. Tamura-Sakaguchi, R.; Aruga, R.; Hirose, M.; Ekimoto, T.; Miyake, T.; Hizukuri, Y.; Oi, R.; Kaneko, M.K.; Kato, Y.; Akiyama, Y., et al. Moving toward generalizable NZ-1 labeling for 3D structure determination with optimized epitope-tag insertion. *Acta Crystallogr D Struct Biol* **2021**, *77*, 645-662, doi:10.1107/s2059798321002527.
38. Kaneko, M.K.; Ohishi, T.; Nakamura, T.; Inoue, H.; Takei, J.; Sano, M.; Asano, T.; Sayama, Y.; Hosono, H.; Suzuki, H., et al. Development of Core-Fucose-Deficient Humanized and Chimeric Anti-Human Podoplanin Antibodies. *Monoclon Antib Immunodiagn Immunother* **2020**, *39*, 167-174, doi:10.1089/mab.2020.0019.
39. Fujii, Y.; Matsunaga, Y.; Arimori, T.; Kitago, Y.; Ogasawara, S.; Kaneko, M.K.; Kato, Y.; Takagi, J. Tailored placement of a turn-forming PA tag into the structured domain of a protein to probe its conformational state. *J Cell Sci* **2016**, *129*, 1512-1522, doi:10.1242/jcs.176685.
40. Abe, S.; Kaneko, M.K.; Tsuchihashi, Y.; Izumi, T.; Ogasawara, S.; Okada, N.; Sato, C.; Tobiume, M.; Otsuka, K.; Miyamoto, L., et al. Antitumor effect of novel anti-podoplanin antibody NZ-12 against malignant pleural mesothelioma in an orthotopic xenograft model. *Cancer Sci* **2016**, *107*, 1198-1205, doi:10.1111/cas.12985.
41. Kaneko, M.K.; Abe, S.; Ogasawara, S.; Fujii, Y.; Yamada, S.; Murata, T.; Uchida, H.; Tahara, H.; Nishioka, Y.; Kato, Y. Chimeric Anti-Human Podoplanin Antibody NZ-12 of Lambda Light Chain Exerts Higher Antibody-Dependent Cellular

Cytotoxicity and Complement-Dependent Cytotoxicity Compared with NZ-8 of Kappa Light Chain. *Monoclon Antib Immunodiagn Immunother* **2017**, *36*, 25-29, doi:10.1089/mab.2016.0047.

42. Ito, A.; Ohta, M.; Kato, Y.; Inada, S.; Kato, T.; Nakata, S.; Yatabe, Y.; Goto, M.; Kaneda, N.; Kurita, K., et al. A Real-Time Near-Infrared Fluorescence Imaging Method for the Detection of Oral Cancers in Mice Using an Indocyanine Green-Labeled Podoplanin Antibody. *Technol Cancer Res Treat* **2018**, *17*, 1533033818767936, doi:10.1177/1533033818767936.
43. Tamura, R.; Oi, R.; Akashi, S.; Kaneko, M.K.; Kato, Y.; Nogi, T. Application of the NZ-1 Fab as a crystallization chaperone for PA tag-inserted target proteins. *Protein Sci* **2019**, *28*, 823-836, doi:10.1002/pro.3580.
44. Kuwata, T.; Yoneda, K.; Mori, M.; Kanayama, M.; Kuroda, K.; Kaneko, M.K.; Kato, Y.; Tanaka, F. Detection of Circulating Tumor Cells (CTCs) in Malignant Pleural Mesothelioma (MPM) with the "Universal" CTC-Chip and An Anti-Podoplanin Antibody NZ-1.2. *Cells* **2020**, *9*, doi:10.3390/cells9040888.
45. Nishinaga, Y.; Sato, K.; Yasui, H.; Taki, S.; Takahashi, K.; Shimizu, M.; Endo, R.; Koike, C.; Kuramoto, N.; Nakamura, S., et al. Targeted Phototherapy for Malignant Pleural Mesothelioma: Near-Infrared Photoimmunotherapy Targeting Podoplanin. *Cells* **2020**, *9*, doi:10.3390/cells9041019.
46. Fujii, Y.; Kaneko, M.; Neyazaki, M.; Nogi, T.; Kato, Y.; Takagi, J. PA tag: a versatile protein tagging system using a super high affinity antibody against a dodecapeptide derived from human podoplanin. *Protein Expr Purif* **2014**, *95*, 240-247, doi:10.1016/j.pep.2014.01.009.
47. Kato, Y.; Kaneko, M.K.; Kunita, A.; Ito, H.; Kameyama, A.; Ogasawara, S.; Matsuura, N.; Hasegawa, Y.; Suzuki-Inoue, K.; Inoue, O., et al. Molecular analysis of the pathophysiological binding of the platelet aggregation-inducing factor podoplanin to the C-type lectin-like receptor CLEC-2. *Cancer Sci* **2008**, *99*, 54-61, doi:10.1111/j.1349-7006.2007.00634.x.
48. Kato, Y.; Vaidyanathan, G.; Kaneko, M.K.; Mishima, K.; Srivastava, N.; Chandramohan, V.; Pegram, C.; Keir, S.T.; Kuan, C.T.; Bigner, D.D., et al. Evaluation of anti-podoplanin rat monoclonal antibody NZ-1 for targeting malignant gliomas. *Nucl Med Biol* **2010**, *37*, 785-794, doi:10.1016/j.nucmedbio.2010.03.010.
49. Heider, K.H.; Sproll, M.; Susani, S.; Patzelt, E.; Beaumier, P.; Ostermann, E.; Ahorn, H.; Adolf, G.R. Characterization of a high-affinity monoclonal antibody specific for CD44v6 as candidate for immunotherapy of squamous cell carcinomas. *Cancer Immunol Immunother* **1996**, *43*, 245-253, doi:10.1007/s002620050329.
50. Heider, K.H.; Mulder, J.W.; Ostermann, E.; Susani, S.; Patzelt, E.; Pals, S.T.; Adolf, G.R. Splice variants of the cell surface glycoprotein CD44 associated with metastatic tumour cells are expressed in normal tissues of humans and cynomolgus monkeys. *Eur J Cancer* **1995**, *31a*, 2385-2391, doi:10.1016/0959-8049(95)00420-3.
51. Gansauge, F.; Gansauge, S.; Zobywalski, A.; Scharnweber, C.; Link, K.H.; Nussler, A.K.; Beger, H.G. Differential expression of CD44 splice variants in human pancreatic adenocarcinoma and in normal pancreas. *Cancer Res* **1995**, *55*, 5499-5503.
52. Beham-Schmid, C.; Heider, K.H.; Hoefler, G.; Zatloukal, K. Expression of CD44 splice variant v10 in Hodgkin's disease is associated with aggressive behaviour and high risk of relapse. *J Pathol* **1998**, *186*, 383-389, doi:10.1002/(sici)1096-9896(199812)186:4<383::Aid-path202>3.0.Co;2-a.
53. Mishra, M.N.; Chandavarkar, V.; Sharma, R.; Bhargava, D. Structure, function and role of CD44 in neoplasia. *J Oral Maxillofac Pathol* **2019**, *23*, 267-272, doi:10.4103/jomfp.JOMFP_246_18.
54. Hirata, K.; Suzuki, H.; Imaeda, H.; Matsuzaki, J.; Tsugawa, H.; Nagano, O.; Asakura, K.; Saya, H.; Hibi, T. CD44 variant 9 expression in primary early gastric cancer as a predictive marker for recurrence. *Br J Cancer* **2013**, *109*, 379-386, doi:10.1038/bjc.2013.314.
55. Shitara, K.; Doi, T.; Nagano, O.; Imamura, C.K.; Ozeki, T.; Ishii, Y.; Tsuchihashi, K.; Takahashi, S.; Nakajima, T.E.; Hironaka, S., et al. Dose-escalation study for the targeting of CD44v(+) cancer stem cells by sulfasalazine in patients with advanced gastric cancer (EPOC1205). *Gastric Cancer* **2017**, *20*, 341-349, doi:10.1007/s10120-016-0610-8.
56. Erb, U.; Megaptche, A.P.; Gu, X.; Büchler, M.W.; Zöller, M. CD44 standard and CD44v10 isoform expression on leukemia cells distinctly influences niche embedding of hematopoietic stem cells. *J Hematol Oncol* **2014**, *7*, 29, doi:10.1186/1756-8722-7-29.
57. Holm, F.; Hellqvist, E.; Mason, C.N.; Ali, S.A.; Delos-Santos, N.; Barrett, C.L.; Chun, H.J.; Minden, M.D.; Moore, R.A.; Marra, M.A., et al. Reversion to an embryonic alternative splicing program enhances leukemia stem cell self-renewal. *Proc Natl Acad Sci U S A* **2015**, *112*, 15444-15449, doi:10.1073/pnas.1506943112.
58. Tang, L.; Huang, H.; Tang, Y.; Li, Q.; Wang, J.; Li, D.; Zhong, Z.; Zou, P.; You, Y.; Cao, Y., et al. CD44v6 chimeric antigen receptor T cell specificity towards AML with FLT3 or DNMT3A mutations. *Clin Transl Med* **2022**, *12*, e1043, doi:10.1002/ctm2.1043.
59. Verel, I.; Heider, K.H.; Siegmund, M.; Ostermann, E.; Patzelt, E.; Sproll, M.; Snow, G.B.; Adolf, G.R.; van Dongen, G.A. Tumor targeting properties of monoclonal antibodies with different affinity for target antigen CD44V6 in nude mice bearing head-and-neck cancer xenografts. *Int J Cancer* **2002**, *99*, 396-402, doi:10.1002/ijc.10369.
60. Li, G.; Suzuki, H.; Ohishi, T.; Asano, T.; Tanaka, T.; Yanaka, M.; Nakamura, T.; Yoshikawa, T.; Kawada, M.; Kaneko, M.K., et al. Antitumor activities of a defucosylated anti-EpCAM monoclonal antibody in colorectal carcinoma xenograft models. *Int J Mol Med* **2023**, *51*, doi:10.3892/ijmm.2023.5221.
61. Nanamiya, R.; Takei, J.; Ohishi, T.; Asano, T.; Tanaka, T.; Sano, M.; Nakamura, T.; Yanaka, M.; Handa, S.; Tateyama, N., et al. Defucosylated Anti-Epidermal Growth Factor Receptor Monoclonal Antibody (134-mG(2a)-f) Exerts Antitumor Activities in Mouse Xenograft Models of Canine Osteosarcoma. *Monoclon Antib Immunodiagn Immunother* **2022**, *41*, 1-7, doi:10.1089/mab.2021.0036.

62. Kawabata, H.; Suzuki, H.; Ohishi, T.; Kawada, M.; Kaneko, M.K.; Kato, Y. A Defucosylated Mouse Anti-CD10 Monoclonal Antibody (31-mG(2a)-f) Exerts Antitumor Activity in a Mouse Xenograft Model of CD10-Overexpressed Tumors. *Monoclon Antib Immunodiagn Immunother* **2022**, *41*, 59-66, doi:10.1089/mab.2021.0048.
63. Kawabata, H.; Ohishi, T.; Suzuki, H.; Asano, T.; Kawada, M.; Suzuki, H.; Kaneko, M.K.; Kato, Y. A Defucosylated Mouse Anti-CD10 Monoclonal Antibody (31-mG(2a)-f) Exerts Antitumor Activity in a Mouse Xenograft Model of Renal Cell Cancers. *Monoclon Antib Immunodiagn Immunother* **2022**, *41*, 320-327, doi:10.1089/mab.2021.0049.
64. Asano, T.; Tanaka, T.; Suzuki, H.; Li, G.; Ohishi, T.; Kawada, M.; Yoshikawa, T.; Kaneko, M.K.; Kato, Y. A Defucosylated Anti-EpCAM Monoclonal Antibody (EpMab-37-mG(2a)-f) Exerts Antitumor Activity in Xenograft Model. *Antibodies (Basel)* **2022**, *11*, doi:10.3390/antib11040074.
65. Tateyama, N.; Nanamiya, R.; Ohishi, T.; Takei, J.; Nakamura, T.; Yanaka, M.; Hosono, H.; Saito, M.; Asano, T.; Tanaka, T., et al. Defucosylated Anti-Epidermal Growth Factor Receptor Monoclonal Antibody 134-mG(2a)-f Exerts Antitumor Activities in Mouse Xenograft Models of Dog Epidermal Growth Factor Receptor-Overexpressed Cells. *Monoclon Antib Immunodiagn Immunother* **2021**, *40*, 177-183, doi:10.1089/mab.2021.0022.
66. Takei, J.; Ohishi, T.; Kaneko, M.K.; Harada, H.; Kawada, M.; Kato, Y. A defucosylated anti-PD-L1 monoclonal antibody 13-mG(2a)-f exerts antitumor effects in mouse xenograft models of oral squamous cell carcinoma. *Biochem Biophys Rep* **2020**, *24*, 100801, doi:10.1016/j.bbrep.2020.100801.
67. Kaneko, M.K.; Ohishi, T.; Kawada, M.; Kato, Y. A cancer-specific anti-podocalyxin monoclonal antibody (60-mG(2a)-f) exerts antitumor effects in mouse xenograft models of pancreatic carcinoma. *Biochem Biophys Rep* **2020**, *24*, 100826, doi:10.1016/j.bbrep.2020.100826.
68. Kato, Y.; Kaneko, M.K. A cancer-specific monoclonal antibody recognizes the aberrantly glycosylated podoplanin. *Sci Rep* **2014**, *4*, 5924, doi:10.1038/srep05924.
69. Kaneko, M.K.; Nakamura, T.; Kunita, A.; Fukayama, M.; Abe, S.; Nishioka, Y.; Yamada, S.; Yanaka, M.; Saidoh, N.; Yoshida, K., et al. ChLpMab-23: Cancer-Specific Human-Mouse Chimeric Anti-Podoplanin Antibody Exhibits Antitumor Activity via Antibody-Dependent Cellular Cytotoxicity. *Monoclon Antib Immunodiagn Immunother* **2017**, *36*, 104-112, doi:10.1089/mab.2017.0014.
70. Kaneko, M.K.; Yamada, S.; Nakamura, T.; Abe, S.; Nishioka, Y.; Kunita, A.; Fukayama, M.; Fujii, Y.; Ogasawara, S.; Kato, Y. Antitumor activity of chLpMab-2, a human-mouse chimeric cancer-specific antihuman podoplanin antibody, via antibody-dependent cellular cytotoxicity. *Cancer Med* **2017**, *6*, 768-777, doi:10.1002/cam4.1049.
71. Suzuki, H.; Kaneko, M.K.; Kato, Y. Roles of Podoplanin in Malignant Progression of Tumor. *Cells* **2022**, *11*, doi:10.3390/cells11030575.
72. Ishikawa, A.; Waseda, M.; Ishii, T.; Kaneko, M.K.; Kato, Y.; Kaneko, S. Improved anti-solid tumor response by humanized anti-podoplanin chimeric antigen receptor transduced human cytotoxic T cells in an animal model. *Genes Cells* **2022**, *27*, 549-558, doi:10.1111/gtc.12972.
73. Chalise, L.; Kato, A.; Ohno, M.; Maeda, S.; Yamamichi, A.; Kuramitsu, S.; Shiina, S.; Takahashi, H.; Ozone, S.; Yamaguchi, J., et al. Efficacy of cancer-specific anti-podoplanin CAR-T cells and oncolytic herpes virus G47Δ combination therapy against glioblastoma. *Molecular Therapy - Oncolytics* **2022**, *26*, 265-274, doi:10.1016/j.omto.2022.07.006.
74. Shiina, S.; Ohno, M.; Ohka, F.; Kuramitsu, S.; Yamamichi, A.; Kato, A.; Motomura, K.; Tanahashi, K.; Yamamoto, T.; Watanabe, R., et al. CAR T Cells Targeting Podoplanin Reduce Orthotopic Glioblastomas in Mouse Brains. *Cancer Immunol Res* **2016**, *4*, 259-268, doi:10.1158/2326-6066.Cir-15-0060.